

Ultrasonic force microscopy for nanometer resolution subsurface imaging

Kazushi Yamanaka and Hisato Ogiso^{a)}

Mechanical Engineering Laboratory, Namiki 1-2, Tsukuba, Ibaraki 305, Japan

Oleg Kolosov^{b)}

Joint Research Center for Atom Technology, Angstrom Technology Partnership, Higashi 1-1-4, Tsukuba, Ibaraki 305, Japan

(Received 10 September 1993; accepted for publication 2 November 1993)

We present a novel method for nanometer resolution subsurface imaging. When a sample of atomic force microscope (AFM) is vertically vibrated at ultrasonic frequencies much higher than the cantilever resonance, the tip cannot vibrate but it is cyclically indented into the sample. By modulating the amplitude of ultrasonic vibration, subsurface features are imaged from the cantilever deflection vibration at the modulation frequency. By adding low-frequency lateral vibration to the ultrasonic vibration, subsurface features with different shear rigidity are imaged from the torsional vibration of cantilever. Thus controlling the direction of vibration forces, we can discriminate subsurface features of different elastic properties.

For the development of nanometer scale electronic and mechanical devices, there is an increasing need for nanometer resolution imaging method of subsurface features (groups of ions, clusters, lattice defects, crystal grains, etc.). Some relating methods have been proposed in scanning force microscopy (SFM) where the tip^{1,2} or the sample^{3,4} is vibrated to modulate the force. The response to the force modulation is measured to image ion implanted layers,¹ embedded wires,² carbon fiber and epoxy composites,³ and Langmuir-Blodgett films.⁴ These methods are characterized by a tip mounting spring with a spring constant comparable to that of the sample. It is sometimes different from the usual AFM requirement for the spring constant to be as small as possible.⁵ In this letter we propose an alternative imaging method, ultrasonic force microscopy (UFM) that employs a tip mounting cantilever much softer than the tip-sample contact rigidity. We vibrate the sample at frequencies much higher than the resonant frequency of the cantilever⁶ and measure the deflection and/or torsional vibration of the cantilever. It gives nanometer resolution elastic or subsurface images, and moreover, discriminates features of different elastic properties, by controlling the direction of vibration forces. We present a general imaging scheme extending our preliminary work,⁷ and an analysis to compare the elastic contrast of the force modulation mode^{3,4} and the UFM. Then, it is verified by imaging two different subsurface features in a highly oriented pyrolytic graphite (HOPG) sample.

We model the AFM with springs and the mass of tip cantilever m as illustrated in Fig. 1. First, the cantilever is displaced by z_c from its free position due to a static repulsive force. When the sample is vibrated at a frequency F lower than the cantilever resonant frequency F_0 , the cantilever is also vibrated following the sample vibration. The tip-sample contact rigidity is expressed as a spring constant s , as a slope

of the force-displacement relation.⁵ If s is approximated by a linear spring, the peak-to-peak cantilever vibration amplitude is given by

$$V = 2z_c \frac{a/z_c}{1+k/s}, \quad (1)$$

where a is the sample vibration amplitude and k is the cantilever spring constant. The amplitude V does not significantly depend upon the spring constant ratio $K = k/s$ representing the relative sample elasticity, when K is varied from 10^{-1} to 10^{-4} (see curves in Fig. 3 labeled $F \ll F_0$.)

In contrast, when the sample is vibrated at ultrasonic frequencies much higher than the cantilever resonant frequency ($F \gg F_0$), the cantilever cannot follow the sample vibration.⁶ When the vibration amplitude exceeds the initial sample compression ($z_s - z_c$), i.e., $a > a_s - z_c = (k/s)z_c$, the tip is detached from the sample for a certain period within one vibration cycle (Fig. 1). During the contact, a repulsive force is acted and the tip is indented into the sample even when the sample is much more rigid than the cantilever [Fig. 2(b)]. If the time dependence of sample vibration is approximated by a triangular function, the averaged repulsive force for one cycle is⁸

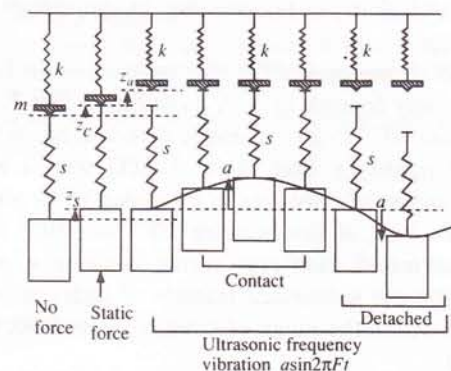


FIG. 1. A spring model for the operation of AFM with sample vibration. See text for the notation of symbols.

^{a)}Also at Joint Research Center for Atom Technology, National Institute for Advanced Interdisciplinary Research.

^{b)}Also at Mechanical Engineering Laboratory, Namiki 1-2, Tsukuba, Ibaraki 305, Japan. On leave from Institute of Chemical Physics of the Russian Academy of Science, Kosygin st. 4, Moscow 117977, Russia.

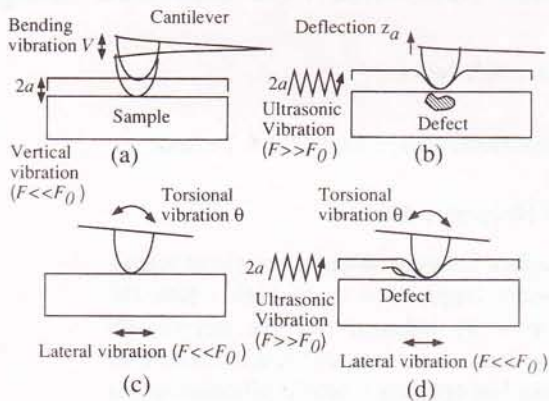


FIG. 2. Imaging schemes of the force modulation modes in AFM and ultrasonic force microscopy. (a) Low-frequency vertical force modulation mode, (b) vertical UFM mode, (c) low-frequency lateral force modulation mode, and (d) lateral UFM mode. F denotes the vibration frequency and F_0 denotes the cantilever resonant frequency.

$$F_m = \frac{s}{4a} \left(\frac{k}{s} z_c + a - z_a \right)^2, \quad (2)$$

where z_a is the additional cantilever deflection due to the vibration (Fig. 1). Since this force is balanced with the cantilever restoring force, i.e., $F_m = k(z_c + z_a)$, z_a is solved as

$$z_a = z_c \left[\frac{k}{s} + \frac{a}{z_c} + 2 \frac{ka}{sz_c} - 2 \sqrt{\frac{ka}{sz_c} \left(\frac{k}{s} + 1 \right) \left(\frac{a}{z_c} + 1 \right)} \right]. \quad (3)$$

For smaller vibration amplitudes, it is shown that $z_a = 0$.

This $z_a(a)$ characteristic is used to define a new imaging method. We measure z_a by switching on and off the vibration, while keeping z_c constant with the vibration switched off. Alternatively, we modulate the vibration amplitude and measure the cantilever deflection vibration at the modulation frequency.⁷ If the modulation is 100% with no feedback of the sample position, the peak-to-peak cantilever vibration amplitude is $V = z_a$. Thus we obtain images representing the elastic property, which we call "vertical" UFM [Fig. 2(b)]. Sometimes, the sample position is feedback controlled to suppress the cantilever deflection fluctuation in frequencies much lower than the modulation frequency. This procedure enables us to obtain a simultaneous approximate topography image and to avoid tip crashing to the sample during the scanning.

It is shown by Eq. (3) that the contrast in UFM images significantly depends upon K as shown in Fig. 3. The change of K from 10^{-4} to 10^{-3} is easily detected. Since the Hertzian contact rigidity s (Ref. 9) of HOPG with a Si_3N_4 tip of 20-nm radius of curvature is estimated to be about 45 N/m for 1-nN load, K lies between 10^{-4} and 10^{-3} for a typical microfabricated cantilever spring constant k of 0.1 N/m. Then, if some subsurface features of different elasticity are located within the range of contact stress field, they can be imaged.

When the sample is laterally vibrated at frequencies lower than the cantilever resonance, torsional vibration of the cantilever is excited by the surface friction force^{10,11} as illustrated in Fig. 2(c), (lateral force modulation). If additional

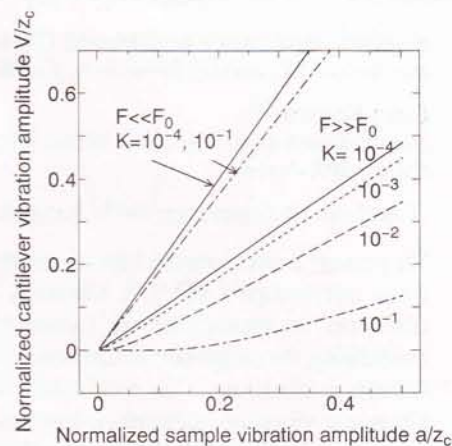


FIG. 3. Calculated cantilever vibration amplitude in the low-frequency vertical force modulation mode ($F \leq F_0$) and the cantilever deflection in the vertical UFM mode ($F \geq F_0$).

vertical ultrasonic vibration of the sample is excited, the torsion torque of the cantilever is changed during the tip is tilted. This torque is sensitive not only to the surface friction, but also to the subsurface shear rigidity, because it is generated during the tip is indented into the sample. Therefore, subsurface features such as a delamination or an edge dislocation that modify the shear rigidity would be imaged by measuring the torsional vibration [Fig. 2(d)]. We call this imaging mode "lateral" UFM.

We conducted the following experiment on a HOPG sample. A piezoelectric transducer was bonded onto a sample holder of an AFM and the sample was glued on the transducer. A 400-nm-thick, 100- μm -long Si_3N_4 cantilever and Si_3N_4 tip with the spring constant of 0.09 N/m and resonant frequency of 40 kHz was used. In the vertical UFM mode, 5.6-MHz ultrasonic vibration of 0.5-nm amplitude was amplitude modulated at 10 kHz.

Figure 4(a) shows a topography image with 500×500 nm field of view and 5.4-nm total height difference, cleaved in an ambient air prior to imaging. Several surface steps were observed. Figure 4(b) shows a low-frequency (10-kHz) vertical force modulation image corresponding to Fig. 2(a). Though the contrast of some edges was enhanced, no significant difference from the topography image was noticed. In a vertical UFM image in Fig. 4(c), a distinct feature of bright bandlike structure, labeled α , was observed between two steps. Since this contrast was not observed in the topography nor in the vertical force modulation image, this contrast seems to have a subsurface origin with different elasticity to vertical forces. It is not surprising that the vertical force modulation image did not show this contrast, because the force modulation mode using a soft cantilever is not sensitive to the variation of elasticity in rigid samples, as described by Eq. (1). It is to be noted that the spatial resolution for this bright feature is better than 10 nm.

Figure 4(d) shows a lateral force modulation image taken at 10 kHz, and the surface steps observed in the topography (a) were enhanced similarly to the edge effect in friction force microscope.¹² when a continuous ultrasonic vibration of 5.6 MHz was added, stringlike features different from

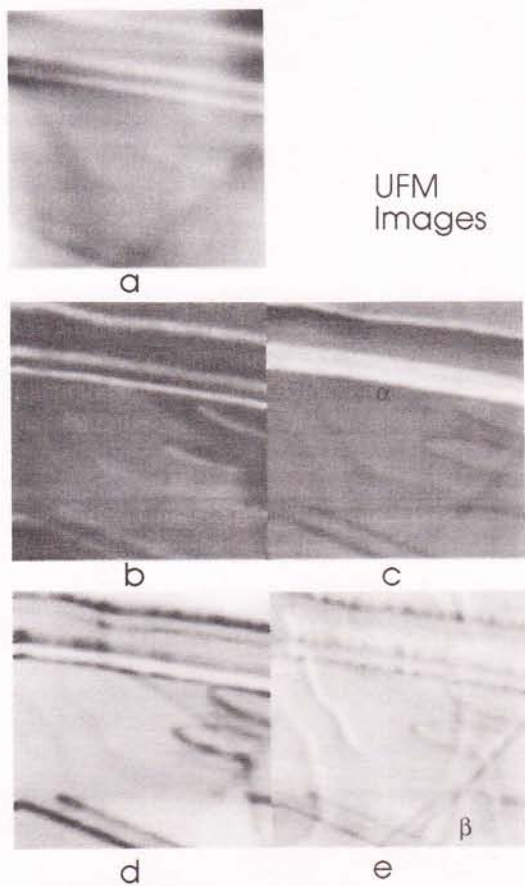


FIG. 4. Images of HOPG. (a) Topography of 500×500 nm area with 5.4-nm total height difference, (b) low-frequency vertical force modulation image, (c) vertical UFM image, (d) low-frequency lateral force modulation image, and (e) lateral UFM image.

the surface steps appeared as labeled β in the lateral UFM image, Fig. 4(e). Since this feature showed an asymmetric contrast consisting of a dark and a bright part, it probably accompanied two sides of small and large shear rigidity. Perhaps, it could be subsurface edge dislocation with extra atomic planes on one side.

Some stringlike features were also slightly visible in the lateral force modulation image (d) and other images, although they were much enhanced in (e). Then, these features do not seem to be completely isolated from the surface, but located near the surface. In contrast, the bright bandlike feature in the vertical UFM image, Fig. 4(c), was completely invisible in other images. Therefore, the bandlike feature probably lies at deeper subsurface than the stringlike features. It is also interesting that they were selectively imaged

in the vertical (c) and lateral (e) UFM images even at the overlapped area. Such an argument suggests a promising performance of the UFM for depth discrimination and defect characterization in subsurface imaging.

The basic feature of the HOPG images was consistently explained by the simple linear spring model. An important implication of Eqs. (1) and (3) is that, if a linear spring is an appropriate model, no contrast reversal is expected between the vertical force modulation image and the UFM image, and a more stiff part should always look brighter than less stiff parts in both kinds of images. Therefore, if a contrast reversal is experimentally observed for a certain feature, other models such as intrinsic nonlinear elasticity would have to be considered. UFM study of this type of object and refinement of the model will be subjects of future works.

In conclusion, we proposed a novel subsurface imaging method with nm resolution, ultrasonic force microscopy that employs vibration of the sample with frequencies much higher than the resonant frequency of cantilever and monitoring the deflection and/or torsional vibration of the cantilever. It can also discriminate features of different elastic properties by controlling the direction of applied forces.

The authors acknowledge partial support of this work from Science and Technology Agency (STA) and National Institute for Advanced Interdisciplinary Research (NAIR) of Japan. They also thank Dr. V. Levin of the Institute of Chemical Physics of Russian Academy of Science, for providing HOPG samples and helpful discussions of their subsurface structure.

- ¹ K. Takata, T. Hasegawa, S. Hosaka, S. Hosoki, and T. Komoda, *Appl. Phys. Lett.* **55**, 17 (1989).
- ² B. Cretin and F. Sthal, *Appl. Phys. Lett.* **62**, 829 (1993).
- ³ P. Maivald, H. J. Butt, S. A. C. Gould, C. B. Prater, B. Drake, J. A. Gurley, V. B. Elings, and P. K. Hansma, *Nanotechnology* **2**, 103 (1991).
- ⁴ M. Radmacher, R. W. Tillmann, M. Fritz, and H. E. Baub, *Science* **257**, 1900 (1992).
- ⁵ G. Binnig, C. F. Quate, and C. Gerber, *Phys. Rev. Lett.* **12**, 930 (1986).
- ⁶ O. Kolosov and K. Yamanaka, *Jpn. J. Appl. Phys.* **32**, L1095 (1993).
- ⁷ O. Kolosov, H. Ogiso, and K. Yamanaka, in *Proceedings of the Internal Research Presentation Meeting of Mechanical Engineering Laboratory, Tsukuba, Japan* (Mechanical Engineering Laboratory, Tsukuba, 1993), Abstract, pp. 19–20.
- ⁸ K. Yamanaka, H. Ogiso, and O. Kolosov (unpublished).
- ⁹ S. P. Timoshenko and J. N. Goodier, *Theory of Elasticity* (McGraw-Hill, London, 1970).
- ¹⁰ S. J. O'Shea and M. E. Welland, *Appl. Phys. Lett.* **61**, 2240 (1992).
- ¹¹ K. Yamanaka, O. Kolosov, H. Ogiso, H. Sato, and T. Koda, in *Proceedings of the Japanese Acoustical Society Spring Meeting* (Japanese Acoustical Society, Tokyo, 1993), p. 889.
- ¹² C. M. Mate, G. M. McClelland, R. Erlandsson, and S. Chaing, *Phys. Rev. Lett.* **59**, 1942 (1987).